

## Thermal and Mechanical Characteristics of EPDM Composites

<sup>1</sup>K.S. Ghase, <sup>2</sup>S.M. El-Marsafy, <sup>3</sup>E.F. Abadeer, <sup>4</sup>A.M. Samir

<sup>1</sup>Ph.D in Chemical Engineering, e-mail: khalednourone@yahoo.com

<sup>2</sup>Professor of Chemical Engineering, Cairo University, e-mail: saharelmarsafy@yahoo.com

<sup>3</sup>Professor of Chemical Engineering, Cairo University, e-mail: ehababadir@hotmail.com

<sup>4</sup>Chemical Engineer, e-mail: amirsamir@hotmail.com

**Abstract:** Ethylene–Propylene–Diene terpolymers (EPDM)-based insulation systems are being widely used as internal thermal insulation for case-bonded solid rocket motors. In this paper, efforts have been made to quantify the effect of fumed silica, basalt fibers, or glass fibers loading on the thermal and mechanical behaviors of EPDM-based thermal insulation. EPDM is compounded with 0, 10, 20, 30 and 40 Phr (parts per hundreds parts of rubber) of fumed silica, basalt fibers, or glass fibers in two roll mill in the presence of organic peroxide varox DBPH-50 as cross linking agent. It has been observed that the addition of fumed silica, basalt fibers, or glass fibers improves the thermal and mechanical performances of the EPDM composites. Also thermal conductivity of the EPDM based composites for thermal insulation significantly decreased with fumed silica or basalt fibers loadings. On the contrary thermal conductivity of the EPDM based composites for thermal insulation significantly increased with glass fibers loadings.

**Key words:** EPDM, Fumed silica, Basalt fibers, Glass fibers, Thermal insulation, Peroxide cross link.

## INTRODUCTION

Nowadays solid rocket propellants are important as they are used in a large application for their simplicity and reliability. Since solid rocket propellants can remain in storage for long periods, and then reliably launch on short notice, they have been frequently used in military applications such as missiles. Solid rocket propellants are assembled with several typical components, as shown in Fig. 1.

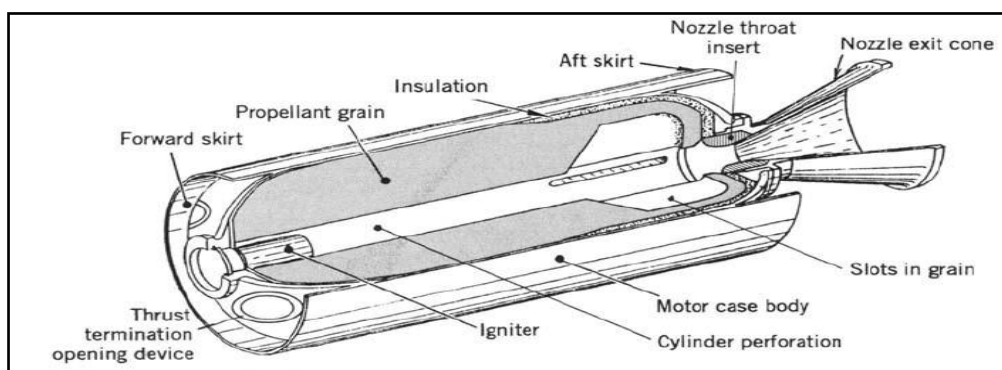


**Fig. 1:** Typical solid rocket motor.

The casing providing the basic structure contains the mass and pressure produced by the burning solid propellant, and transfers thrust to the payload. Typically, the case is internally insulated more to protect the motor structure from adverse heat effects from combustion gases than to prevent heat loss.

The converging-diverging nozzle converts the heat, pressure, and mass flow into thrust. The converging section provides a smooth transition from the spherical aft dome of the case to the nozzle entrance. The diversion section is conical and the throat diameter is sized to target a specific maximum pressure. The average thickness along the nozzle wall does increase near the throat for added thermal structure capability, as shown in Fig. 2.

An igniter, which produces high mass and heat flux, is required to start the solid propellant burning. Finally, the solid propellant, or grain, is the fuel that produces heat, pressure, and mass flow. Solid propellants tend to be quite stable at ambient temperatures and pressures and it is only after the application of an adequate ignition source to the grain surface that the fuel begins to combust sustainably. The fuel/oxidizer/binder mixture casts directly in the case and is left to cure, or can be extruded, cured, and later installed in the case. The cured solid

propellant is called the propellant grain. The grain's internal surface can be machined but is usually formed by allowing the mixture to cure around a forming core. The internal surface of the grain is designed to create a specified pressure and thrust versus time profiles depending on the purpose of the rocket system (Stephen Scot Moore, 2010).

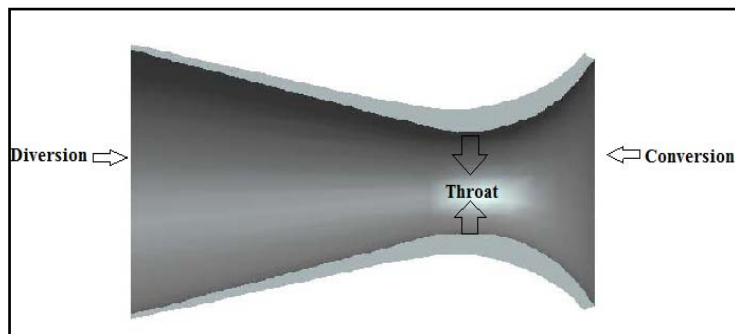


**Fig. 2:** Nozzle geometry.

Throughout the history of rocketry, the performance of rocket-powered devices has depended upon their ability to withstand the high temperatures and loads associated with their use. As the use of rockets has developed to require longer flights, the focus of researches have shifted from developing the most efficient pressure vessel to improving the nozzle, insulation, and other time-sensitive materials. To allow the use of more standard materials for rocket casings, an effective thermal protection system is important (Steven A. Kyriakides, 2009). Elastomers are globally used as thermal insulators for solid rocket motors. The insulator protects the rocket motor from high-temperature gases and particle streams generated by the propellant combustion. The insulator should have high tensile strength and elongation to absorb the mechanical stresses induced to the rocket motor during propellant casting, storage, transportation, and flight. It also helps in anchoring the propellant mass to the inner wall of a rocket motor.

One of the synthetic elastomers concerned in this study is Ethylene-Propylene Diene terpolymer (EPDM) rubber, which is a terpolymer of ethylene, propylene and a non-conjugated diene, having the highest consumption rate amongst all speciality rubbers in the past three decades. The main attributes of EPDM elastomer are its outstanding resistance to oxidation, ozonisation, and weathering effects. EPDM rubber has the lowest specific gravity among all rubbers. The most important properties are its long shelf life and excellent low-temperature properties. Due to these attractive properties of EPDM, it is replacing all other elastomers like nitrile, styrene-butadiene, polydimethyl siloxane, etc. as insulators in an advanced solid booster such as space shuttle of NASA and inertial upper stage motors (Bhuvaneswari, C.M., 2008). One of the most famous insulators is that using asbestos mixed with EPDM. Now the use of this insulator has been brought into question because of the health hazards associated with asbestos.

The present study aims at developing a new rocket motor insulator containing non asbestos fillers. Efforts have been made to quantify the effect of fumed silica, basalt fibers, or glass fibers loading on the thermal and mechanical behaviors of EPDM-based thermal insulation.

## **2. Methodology:**

Thirteen samples were prepared and tested as follows:

## **3. Experimental Work:**

### **3.1 Materials:**

#### **3.1 The Matrix:**

Nordel IP 4640 is an amorphous EPDM grade designed for molded and extruded applications. Higher ethylene content gives more green strength (high elongation in the uncured state) which can help the rubber processor in the mill mixing. However, high ethylene content gives poorer low temperature properties.

#### **3.2 Curative:**

An EPDM insulator formulation is cured with organic peroxide varox DBPH-50. Peroxides typically react with the elastomer chains by removing hydrogen atoms from the carbon backbone of the polymer, thus creating highly active sites on the chain, called radicals, which attach to a similar site on another chain, creating a carbon to carbon cross-link, which is stronger than a sulfur carbon link and more thermally stable. When compared with sulphur curatives, peroxides provide better heat ageing properties, compression set, and better ageing characteristics (Andrew Ciesielski, 1999).

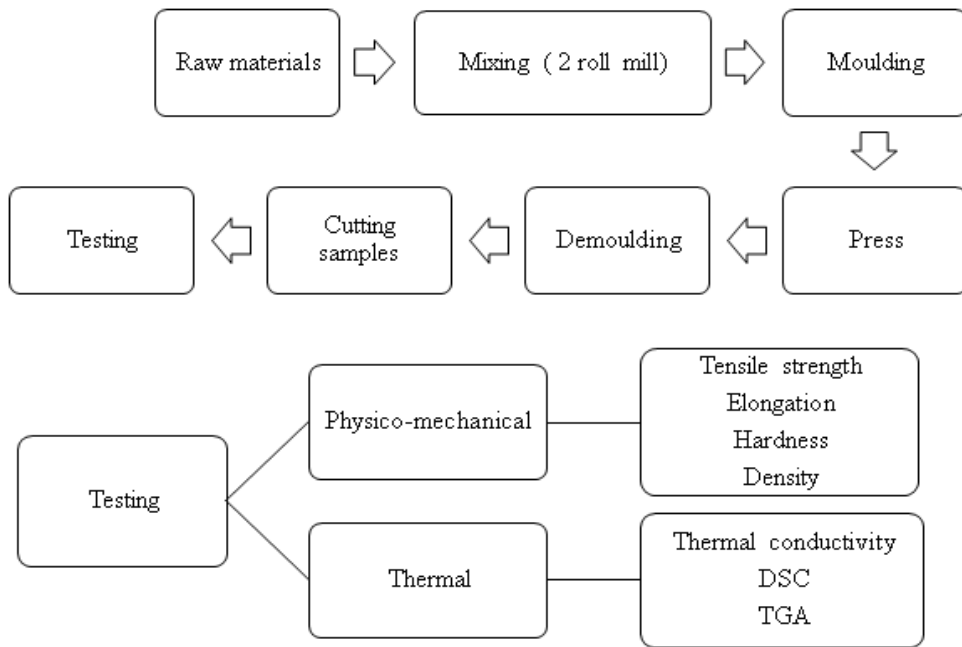


**Fig. 3:** Scheme of work.

### 3.3 Flame Retardant:

The elastomeric insulating compositions include flame retardants selected from chlorinated compounds, antimony trioxide (synergistic flame retardant) and their combinations. Chlorinated organic compounds can be used with antimony trioxide or hydrated alumina to enhance flame retardance. One of the chlorinated hydrocarbons used for this purpose is dechlorane plus 515 (flame retardant) (Bhuvaneswari, C.M., 2006).

### 3.4 Filler:

The non toxic fillers considered in the current study are fumed silica, basalt fibers, and glass fibers. High levels of reinforcing particulate fillers (up to 40 % by weight of the elastomeric insulating materials) can be used for suitably tailoring the modulus (Bhuvaneswari, C.M., 2004). The use of fumed silica (aerosil R972) from Evonik Degussa GmbH as particulate filler would be investigated. Basalt fiber is a material made from extremely fine fibers of basalt. Basalt fibers may vary in diameter from approximately 5µm to approximately 25µm. Preferably, the fibers used in this study are greater than 5µm in diameter as this is far enough above the respiratory limit to make basalt fiber a suitable replacement for asbestos. Basalt fibers are available from commercial sources such as Fiberand Corp., Albarrie Canada Ltd., and under the brand name BASALTEX® from the Masureel Group. The use of glass fibers (supraplast SK660) from SWC Duroplasttechnologie would be investigated. Efforts have been made to quantify the effect of fumed silica, basalt fibers, or glass fibers loading on the thermal and mechanical behaviors of EPDM-based thermal insulation.

Normally, composition of insulation consists of EPDM (4640) as the main matrix mixed with varox DBPH-50 (cross-linking), antimony trioxide (synergistic flame retardant), dechlorane plus 515 (flame retardant), and (fumed silica, basalt fibers, or glass fibers) as fillers. A typical formulation for EPDM insulation is given in Table 1.

**Table 1:** A typical formulation for EPDM insulation.

Sample	Parts per hundred (phr)						
	EPDM	Varox	Dechlorane	Antimony trioxide	Fumed silica	Basalt fibers	Glass fibers
S1	100	2.5	40	20	-	-	-
S2	100	2.5	40	20	10	-	-
S3	100	2.5	40	20	20	-	-
S4	100	2.5	40	20	30	-	-
S5	100	2.5	40	20	40	-	-
S6	100	2.5	40	20	-	10	-

### 3.2 Testing:

#### 3.2.1 Physico-Mechanical Tests:

The physico-mechanical properties under investigation in this study are tensile strength, elongation, hardness, and density. In this paper three types of physico-mechanical testing machines were used. The first test machine is extensometer 10 KN with alpha-technologies T2000 (software) was applied to investigate the tensile

strength and elongation. The second test machine is zwick hardness tester type 3102 was applied to investigate the hardness. The third test machine is sartorius analytical balance was applied to investigate the relative density.

**Table 1:** A typical formulation for EPDM insulation (continued).

Sample	Parts per hundred (phr)						
	EPDM	Varox	Dechlorane	Antimony trioxide	Fumed silica	Basalt fibers	Glass fibers
S7	100	2.5	40	20	-	20	-
S8	100	2.5	40	20	-	30	-
S9	100	2.5	40	20	-	40	-
S10	100	2.5	40	20	-	-	10
S11	100	2.5	40	20	-	-	20
S12	100	2.5	40	20	-	-	30
S13	100	2.5	40	20	-	-	40

### 3.2.2 Thermal Tests:

#### 3.2.2.1 Thermal Conductivity:

Thermal conductivity was measured by using the Lee's Disc apparatus which consists of three cylindrical slabs of copper disc labeled A, B and C, and on each slab, of which a hole is bored to give way for water heater. Jointed rods with low thermal conductivities and a heavy support are to carry the experiment. Other apparatus used are stopwatch, micro screw gauge, thermometers, water and scale balance. In setting up the Lee's disk apparatus, the jointed rods are placed on the heavy stand and screwed firmly to it. One of the cylindrical copper metal disc A was placed on it with two thermometers in the separate holes bored in the disk A and B. Steam from a conical flask was allowed to pass through the cylinder A and temperature  $T_1$  and  $T_2$  were recorded at steady state of about 60 seconds. This is the temperature at which the heat loss through samples to disc B is equal to the heat gained by the sample from disc A.

At steady state,  $T_1$  and  $T_2$  are interchanged and then recorded. Metal disc A is now removed and a bunsen flame is applied at the slab surface until  $T_2$  recorded the temperature up to 10°C higher than the temperature at steady state at 30 minutes interval until the temperatures fall again to about 10°C below the steady state temperature. The above procedure was repeated for each sample. The cross section area for each sample was determined while the beam balance was used to get the mass of the disc A. A cooling curve was plotted for each sample and the slope was determined. Then, the thermal conductivity (K) of each sample was determined using a relation of the form:

$$\frac{K\pi D^2}{4} \frac{(Q_1 - Q_2)}{I} = M \times C \times (\text{Slope}) \quad (1)$$

Where K is the thermal conductivity to be determined, I is the thickness of the sample, M is the mass of the disc A, C is the specific heat capacity of disc A (copper).  $Q_1 - Q_2$  is the temperature difference and  $\pi D^2/4$  is the cross-section area of molded circular sample with diameter D (Adenodi, R.A., B.F. Akinwale, 2009).

#### 3.2.2.2 Differential Scanning Calorimeter (DSC):

The energy changes that occur as a sample is heated cooled or held isothermally, together with the temperature at which these changes occur were measured using a DSC analyzer Shimadzu – 50 –Japan.

#### 3.2.2.3 Thermo Gravimetric Analysis (TGA):

TGA is an experimental technique in which the weight or, strictly speaking, the mass of a sample is measured as a function of sample temperature or time. The sample is typically heated at a constant heating rate or held at a constant temperature (isothermal measurement). A TGA analyzer Shimadzu – 50 –Japan is used for this test.

## RESULTS AND DISCUSSION

All tests are repeated three times for each sample and their average value is recorded.

### 4.1 Tensile Strength:

Fig. 4. shows that increasing the amount of added fillers, increases the tensile strength of the insulator. This increase followed the order fumed silica > glass fiber > basalt fiber. This can be attributed to the fact that silica is classified as an excellent reinforcement filler for plastics, which is highly compatible with plastics used in insulation. And basalt itself is a fiber characterized by its high tensile strength. Also glass fiber is characterized by its high tensile strength. Also an important note, that the values of tensile strength for fumed silica are higher than other values of different filler types. This happens because fumed silica is a very fine solid powder with a very high order of adhesion with the matrix. Other types of fillers are fibrous having high aspect ratio and

random distribution with the matrix, which exerts greater viscous drag on polymer to aid in molecular alignment.

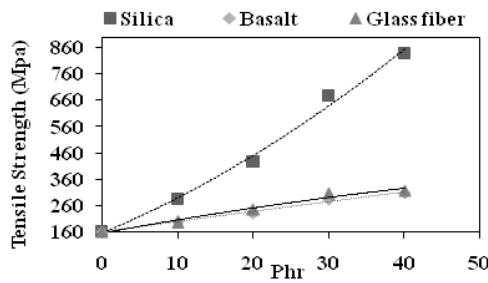


**Fig. 4:** Effect of the ratio of phr additives on the tensile strength of the insulator.

#### 4.2 Elongation:

The values of the elongation in % are shown in Fig. 5.

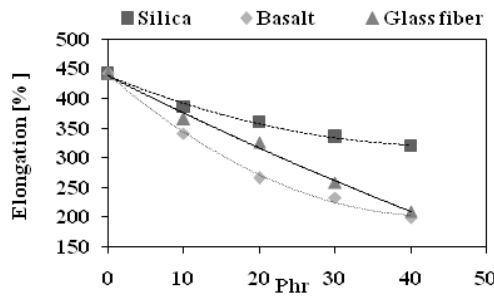


**Fig. 5:** Effect of the ratio of phr additives on the elongation of the insulator.

It is apparent from Fig. 5. that increasing the amount of added fillers, results in lower elongation. It is a rare occurrence for elongation at the yield point to be increased by increasing the amount of a filler. This is attributed to the fact that stress whitening occurs almost immediately on elongation of composites containing higher filler concentrations, or when the filler consists of a large particles. In both cases, the matrix is restricted in its ability to stretch between packed particles or around large particles, and de-wetting or de-bonding of the particles causes cavitation, which appears as stress whitening. Smaller particles at low concentrations are freer to move with the matrix, and correspondingly, the matrix is freer to stretch around them. The viscous drag of small particles with good adhesion to the matrix can then produce an apparent strength improvement and, resulting in higher ultimate elongation. As it is observed in (10 and 20) phr of fumed silica. If the interfacial bond exceeds the matrix strength, the matrix is less free to draw around the particles, and lower elongation and higher strength results. As it is observed in other types of filler.

#### 4.3 Hardness:

The values of the hardness for each of the thirteen formulations under study are shown in Fig. 6.

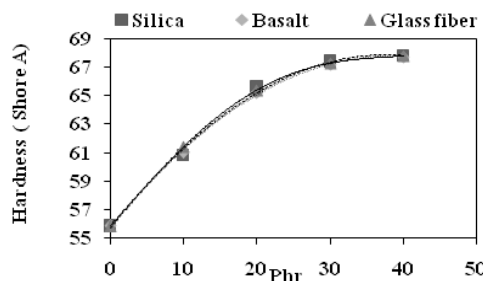


**Fig. 6:** Effect of the ratio of phr additives on the hardness of the insulator.

It is exhibited in the figure that increasing the amount of added fillers, results in higher values of hardness. This can be attributed to the fact that solid fillers always increase the modulus of a composite (as in fumed silica). Also Fillers which increase the moduli of composites generally will increase hardness, as in fibers (glass

fibers and basalt fibers), where the filler aspect ratios is greater than about (2 to 1), leading to increase the moduli (Katz, H.S., 1978).

#### 4.4 Density:

Fig. 7. shows that increasing the amount of added fillers, results in higher density. This is due to the fact that density of fumed silica, basalt fiber, and glass fiber are higher than the density of EPDM.

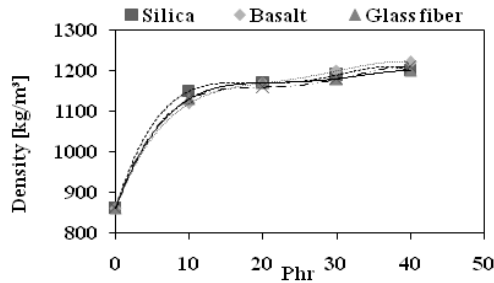


**Fig. 7:** Effect of the ratio of phr additives on the density of the insulator.

#### 4.5 Thermal Conductivity Measurement:

Fig. 8. reveals that increasing the amount of added fumed silica or basalt fibers as fillers, results in lower thermal conductivity. This may be attributed to the fact that the thermal conductivity of basalt fibers (0.031 w/m.<sup>o</sup>K) and fumed silica (0.04 w/m.<sup>o</sup>K) is lower than the thermal conductivity of EPDM. On the contrary increasing the amount of added glass fibers as filler, results in higher values of thermal conductivity. This can be attributed to the fact that the thermal conductivity of glass fiber (0.7 W/m.<sup>o</sup>K ) is higher than the thermal conductivity of EPDM.

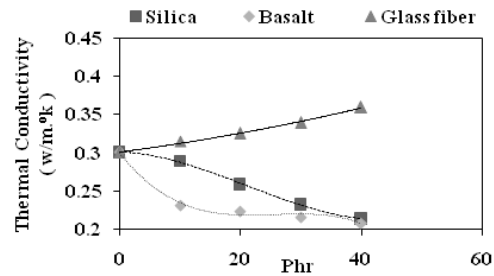


**Fig. 8:** Effect of the ratio of phr additives on the thermal conductivity of the insulator.

#### 4.6 DSC:

Observing and analyzing Figs. 9-11, which represent the values of  $T_g$  ,  $T_c$  and  $T_d$ , it is noticed that increasing the amount of added filler, results in higher  $T_g$  ,  $T_c$  and  $T_d$ . Where  $T_g$  is the glass transition temperature,  $T_c$  is the crystallization temperature, and  $T_d$  is the decomposition temperature.

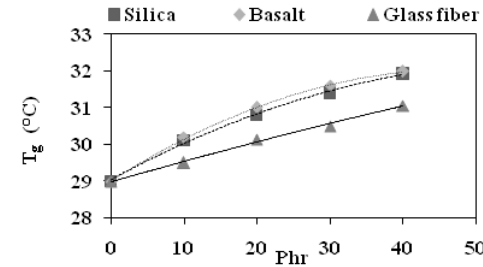


**Fig. 9:** Effect of the ratio of phr additives on  $T_g$

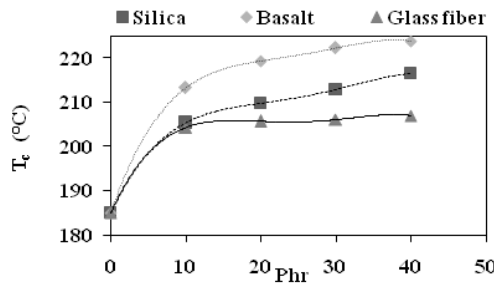


**Fig. 10:** Effect of the ratio of phr additives on  $T_c$

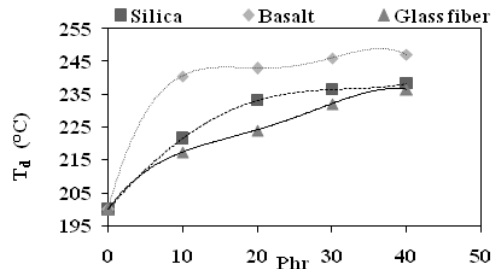


**Fig. 11:** Effect of the ratio of phr additives on  $T_d$

#### 4.7 TGA:

Observing and analyzing Figs. 12 and 13. which represent the values of  $T_i$  and  $T_f$ , show that increasing the amount of added filler, results in higher  $T_i$ ,  $T_f$ .

Where:

$T_i$ ..... is initial decomposition temperature.

$T_f$ ..... is final temperature decomposition.

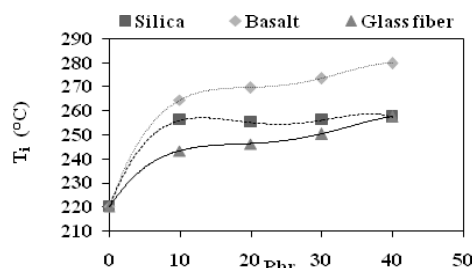


**Fig. 12:** Effect of the ratio of phr additives on  $T_i$

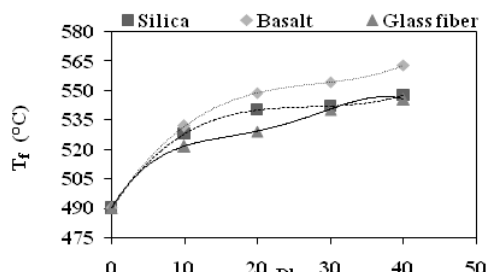


**Fig. 13:** Effect of the ratio of phr additives on  $T_f$

#### 5. Conclusion:

In order to develop a new rocket motor insulator containing non asbestos fillers, efforts have been made to quantify the effect of fumed silica, basalt fibers, or glass fibers loading on the thermal and mechanical behaviors of EPDM-based thermal insulation. Results presented in this paper show that on loading EPDM rubber with various formulations of fumed silica, basalt fibers, or glass fibers the physico- mechanical properties were appreciably improved. Thermal stability of the EPDM composites was significantly enhanced. Also the thermal conductivity was lowered by using fumed silica or basalt fiber as fillers. On the contrary using of glass fiber as

filler increased the thermal conductivity of EPDM-based thermal insulation which is not desirable as far as space applications are concerned.

## REFERENCES

Adenodi, R.A., B.F. Akinwale, 2009. "Analysis of Thermal and Electrical Properties of Some Clay Samples," Electronic Journal of Geotechnical Engineering, (2009), 14, <http://www.ejge.com/2009/Ppr09131/Ppr09131.pdf>.

Andrew Ciesielski, 1999. "An Introduction to Rubber Technology," Rapra Technology Limited, ISBN: 1-85957-150-6.

Bhuvaneswari, C.M., M.S. Sureshkumar, S.D. Kakade and Manoj Gupta, 2006. "Ethylene-propylene Diene Rubber as a Futuristic Elastomer for Insulation of Solid Rocket Motors," Defense Science Journal, (January 2006), 56(3): 309-320.

Bhuvaneswari, C.M., M.S. Sureshkumar, V.D. Deuskar and Kakade, 2004. "EPDM blends-as a potential candidate for thermal insulation of case-bonded solid rocket motors," In Seminar of Society of Polymer Science, 26 July 2004, Pune.

Bhuvaneswari, C.M., S.D. Kakade, V.D. Deuskar, A.B. Dange, Manoj Gupta, 2008. "Filled Ethylene-Propylene Diene Terpolymer Elastomer as Thermal Insulator for Case-Bonded Solid Rocket Motors," Defense Science Journal, (January 2008), 58(1): 94-102.

Katz, H.S., 1978. "Hand Book of Fillers and Reinforcements for Plastics," New York, Van Nostrand Reinhold Company, ISBN: 0-442-25372-9.

Stephen Scot Moore, 2010. "Ballistics Modeling Combustion Heat Loss Through Chambers and Nozzels of Solid Rocket Motors," MSc, California State University, Sacramento.

Steven A. Kyriakides, Scott W. Case, 2009. "Processing Mechanical Test Specimens of Charred Solid Rocket Motor Insulation Materials," Journal of Spacecraft and Rockets, November–December, 46(6).